IEEE Photonics Journal
An IEEE Photonics Society Publication

Open Access

IR Image Upconversion Under Dual-Wavelength Laser Illumination

Volume 8, Number 6, December 2016

H. Maestre
A. J. Torregrosa, ***Member, IEEE***
J. Capmany, ***Senior Member, IEEE***

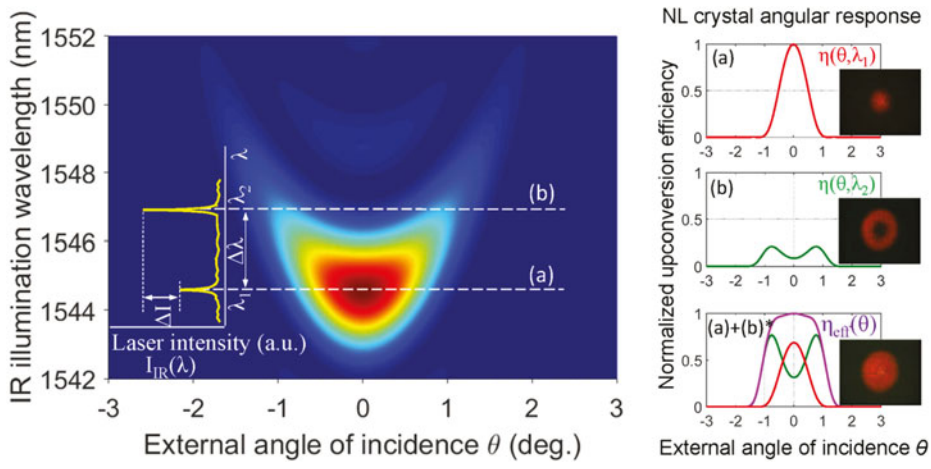

DOI: 10.1109/JPHOT.2016.2630852
1943-0655 © 2016 IEEE

IR Image Upconversion Under Dual-Wavelength Laser Illumination

H. Maestre, A. J. Torregrosa, *Member, IEEE*, and J. Capmany, *Senior Member, IEEE*

Department of Communications Engineering, Universidad Miguel Hernandez, Elche (Alicante) E03202, Spain

DOI:10.1109/JPHOT.2016.2630852

Manuscript received September 9, 2016; revised November 14, 2016; accepted November 16, 2016. Date of publication November 21, 2016; date of current version December 7, 2016. This work was supported by the European Union and the Government of Spain through project TEC2014-60084-R. Corresponding author: H. Maestre (e-mail: hmaestre@umh.es).

Abstract: We investigate the use of dual-wavelength laser illumination in a nonlinear infrared-to-visible image upconversion system. We show how a two-wavelength laser illumination can combine the enhanced upconversion field-of-view (FOV) characteristic of broadband thermal or amplified spontaneous emission (ASE) illumination with the higher power intensity of a laser. By properly choosing the wavelength spectral spacing of only two laser wavelengths and their relative amplitudes, the FOV that can be upconverted in the nonlinear crystal can be enlarged up to an extent similar to broadband illumination and intensity homogenized. In this way, a step is taken towards image upconversion beyond the lab to practical longer range illumination-assisted outdoor applications. We provide an experimental verification in good agreement with our model's simulations for original infrared images in the eye-safe spectral region around 1550 nm upconverted to around 631 nm in a periodically poled $LiNbO_3$ crystal.

Index Terms: Imaging systems, solid-state lasers, nonlinear crystals, optics.

1. Introduction

Nonlinear wavelength upconversion of 2-D images based on sum-frequency mixing (SFM) with a pump laser beam [1] is regaining research interest lately, in particular, in the continuous wave due to the conversion efficiency enhancement provided by combining intra-cavity mixing in the pump laser [2] and the high effective nonlinear coefficient of poled ferroelectric crystals for second-order nonlinear interactions [3]. In this way, un-scanned full 2-D images in the infrared can be upconverted in real time to the visible where widespread focal plane array (FPA) detectors such as silicon-based CCD or CMOS are well developed with better characteristics in terms of noise, speed, resolution, or uncooled operation when compared to other existing imaging sensors in different spectral ranges of the infrared and in the THz region [4], [5].

One of the limiting factors under single-wavelength illumination is the reduced field-of-view (FOV) that can be upconverted [6]. By FOV, we refer here to the span of IR directions around the axis of an imaging centered optical system. This limitation arises from the narrow angle tolerances typical of phase- or quasi-phase matching, as image formation relies on the existence of non-collinear upconversion interactions inside a nonlinear (NL) crystal [7]. It has been shown that broadband illumination of targets leads to a significant enhancement of the upconverted FOV as compared with narrowband laser illumination [8]. Taking advantage of the larger set of IR wave-vectors available

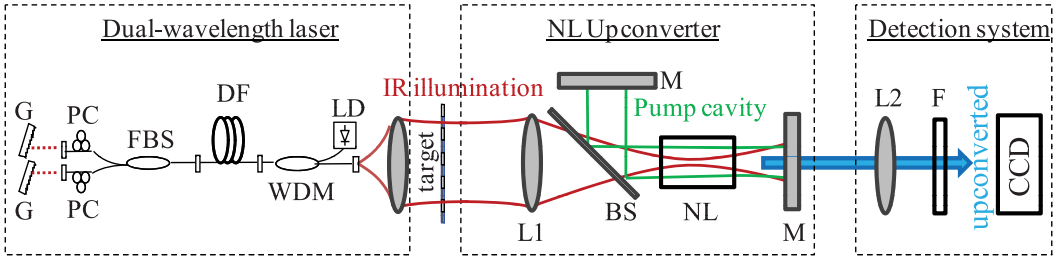

Fig. 1. Experimental setup for IR image upconversion using an IR dual-wavelength laser as the illumination source. The dashed boxes represent the main building blocks of the upconversion system.

under broadband illumination, the span of angles at which efficient non-collinear interactions can be significantly increased. However, broadband illumination sources do not provide as much peak power or intensity as laser sources in general, thus leading to lower nonlinear upconversion efficiency. Most present and previous work on image upconversion has been carried out in the lab using small targets and illumination spots on the order of a few cm, where typically thermal or ASE sources can provide enough illumination intensity for efficient upconversion [7]–[10]. Extending the possibility of upconversion to longer-range outdoor applications requires, however, a high long-range illumination level on a wider area, which is most conveniently achieved with laser illumination. It is worth then to investigate whether the beneficial enhancement in FOV provided by broadband illumination can be easily combined with the high power density of laser illumination.

Upconversion of laser illuminated targets is of interest in lidar and pulsed illumination systems where a high number of photons are available and hence objects placed at long distances can be efficiently upconverted. An enhancement in the field-of-view is of interest since it is equivalent to a wider upconverted area, thus allowing the acquisition of larger images. In [11], the FOV of an upconverted lidar system was enhanced with a microlens array. Here, we show that upconversion based on laser illumination with only two quite close different wavelengths could prove very useful for longer range outdoor applications with wider FOV. However, as discussed below, a suitable choice of the wavelength spacing and their relative power is required to keep a wider FOV. We focus on eye-safe laser illumination around 1550 nm in order to target outdoor applications. Although dual-wavelength laser applications have been proven in a wide range of scientific and technological areas such as interferometry, sensing, and photonic terahertz (THz) and microwave generation among others [12]–[14], dual-wavelength lasers have not been yet explored in imaging upconversion systems. Commonly, an image up converter is based on a 4-f Fourier optical processing system [3]–[11]. In reference to Fig. 1 (NL Upconverter and Detection system blocks), a single positive lens (L1) collects the points of a full IR image located in its object focal plane, (Target) and collimates them. Subsequently, the wave-vectors at different directions or angles of the IR image mix with the wave-vector of a pump laser beam inside a nonlinear crystal (NL) yielding a collimated upconverted image with an angle demagnification of $\lambda_{up}/\lambda_{IR}$ that is then collected by a second positive lens (L2). This second lens focuses the upconverted image points onto a FPA detector located at its image focal plane (CCD). Equivalently, a collimated beam entering the system can be regarded as an IR image in the focal plane of L1 corresponding to its cross sectional area, and where the different focusing angles of L1 represent different points in the focal plane of L1. Because different spatial portions of the IR image (or IR beam) enter the NL crystal at different angles, the crystal angular tolerance for non-collinear nonlinear interactions determines the span of incoming IR angles, that can be more efficiently upconverted. This, in turn, sets a limit in the spatial portion of the IR image that can be upconverted and, ultimately, on the overall system resolution. Thus, any increase in the FOV of the system becomes beneficial.

2. Experimental Setup

The overall configuration of the system for IR image upconversion using a dual-wavelength laser is plotted in Fig. 1. In order to exploit non-collinear quasi-phase matching (NCQPM), which is

wavelength sensitive, we constructed a tunable dual-wavelength laser comprised of an Er-doped fiber (DF) as the gain medium pumped by laser diode (LD) at 980 nm by means of a dichroic fiber coupler (WDM), a fiber beam splitter (FBS) providing two different feedback paths, two diffraction gratings (G) for independent wavelength tuning and two polarization controllers (PC) for matching the laser polarization to that required for type-0 QPM in the NL crystal. The adjustment of the diffraction gratings allows selecting for each wavelength either its spectral position (horizontal tilt) or its relative amplitude (vertical tilt). The upconverter is based on intracavity sum-frequency mixing (SFM) in a modified paraxial 4f-system with a periodically-poled lithium niobate (PPLN) crystal placed in the Fourier plane (see [8] for details). As illumination, the dual-wavelength IR beam ($\sim$1550 nm) is directed to the object (target) to be imaged and after being modulated by the spatial information of the object, the resultant beam is both focused by the lens L1 into the QPM NL crystal and coupled into the laser cavity of the upconverter system by means of a dichroic beamsplitter (BS). The NL crystal is a 5% MgO-doped periodically-poled $LiNbO_3$ crystal with 3 mm $\times$ 1 mm cross-section, 5 mm long and a poling period $\Lambda = 11.8$ μm (HC Photonics Corp.). A second beam acting as a pump at $\sim$1064 nm (which does not travel through the focusing lens L1) is generated inside a Nd^{3+}:GVO_4 linear-cavity laser formed by two high reflectivity mirrors (M), and interacts in the NL crystal with the focused IR beam in a SFM process. Then, the upconverted radiation ($\sim$630 nm) is collected by the lens L2 and imaged onto an image sensor (CCD) after filtering (F) the remaining IR, SFM and 1064 nm laser pumps and other possible harmonics. This configuration allows independent control of the waist of the interacting beams. For resolution purposes, the pump beam, which acts as a soft aperture with a gaussian spatial profile in the Fourier plane (spatial filter), should be as wide as possible in comparison to the IR beam in order to permit a high number of IR spatial frequencies to pass. This condition is also bounded to the achievable FOV since for a tightly focused illumination beam the set of incoming angles into the NL crystal increases and, in order to preserve the upconverted area, the need of an extended angular response of the NL medium arises. In the next section we provide deeper insight on FOV widening, and we develop a brief theoretical model for predicting the angular response of the upconverter under dual-wavelength illumination.

3. FOV Enhancement

In upconversion by means of a single-wavelength laser illumination the NL crystal angular upconversion response is restricted to an almost collinear interaction with the pump laser beam, with its upconversion efficiency peaking at normal incidence, and a width typically clipping the incoming IR angular span by quasi-phase matching (QPM) angle tolerance, hence limiting the achievable FOV [8]. In previous works, it was shown how broadband illumination can enhance significantly the upconverted FOV in comparison with single-wavelength illumination, due to the multiplicity of different IR wave-vectors available for non-collinear interactions [8], [15]. However, as we discuss next, illumination with dual-wavelength laser radiation suffices to obtain a similar FOV enhancement. For wavelengths other than that of perfect QPM, the NL crystal upconversion angular response changes. Shorter wavelengths keep maximum upconversion at normal incidence although their peak efficiency is sensitively lowered. For longer wavelengths, the peak upconversion efficiency in the NL crystal remains, but it shifts to different angles, i.e., to non-collinear interactions. In a strict sense, this situation does not stem for all wavelengths above perfect QPM, since the actual angular response of the up-converter is the product of the NL crystal angular response and the IR angular spectrum of the focused incoming light. For wavelengths above QPM the peak response shifts to different angles but at the expense of a lower conversion efficiency. Consequently, dual-wavelength illumination would yield an increased upconverter field of view by taking advantage of the overlap of a wavelength at perfect QPM angular response [see Fig. 2(a)] and the angular response at a longer wavelength [Fig. 2(b)], after adequately equalization of the intensity of these wavelengths is applied. These features are dependent upon the upconverter parameters (IR focusing lens and NL crystal length). Therefore, for a given upconverter, the spectral properties of the dual-wavelength laser (ΔI $\equiv$ intensity difference and $\Delta\lambda$ $\equiv$ wavelength spacing) can be selected to tailor the

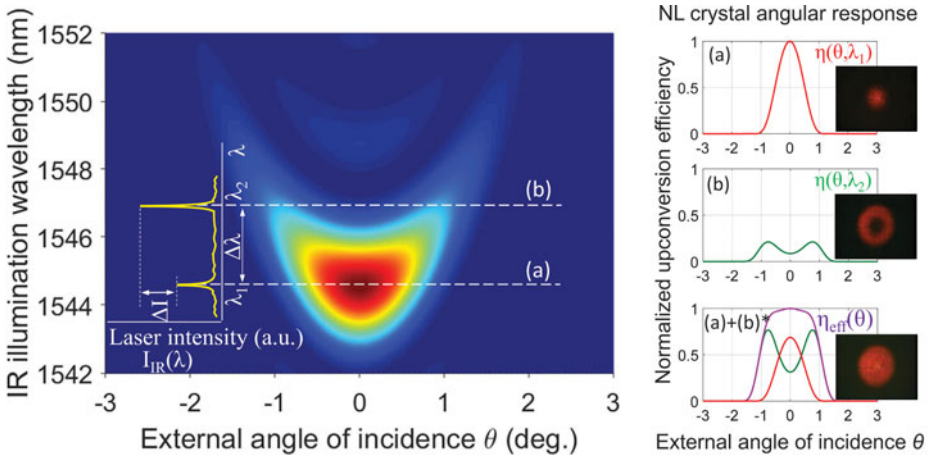

Fig. 2. (Left) Normalized upconversion efficiency as a function of IR illumination wavelength and angle of incidence into the NL crystal. (a) and (b) are the NL angular responses for λ_1 (λ_{QPM}) and λ_2, respectively. (a)+(b)* is the equalized overlap of patterns (a) and (b).

effective angular response of the upconverter, $\eta_{\text{eff}}(\theta)$, by means of the opportunistic combination of upconverted profiles [see Fig. 2(a)+(b)*]. The asterisk is intended to emphasize that the intensity of the longer wavelength (λ_2) was increased for achieving a smooth and broad effective angular response. Calculation in Fig. 2 was performed assuming an IR illumination beam focused to a spot of 40 μm and a 5 mm long MgO:PPLN (MgO-doped periodically-poled Lithium Niobate) crystal at 22 $^{\circ}$C. The insets correspond to the visible upconverted beam profiles recorded in a CCD camera for experimental conditions approaching to the simulation parameters.

The enhancement of the FOV under dual-wavelength illumination can also be treated theoretically. If we assume all interacting waves propagate in z-direction, the image information is contained in the transverse spatial coordinates (x and y). For an input IR beam of spatial field distribution $E_{IR}(x, y)$, lens L1 will transform it to its spatial Fourier transform $E_{IR}(k_x, k_y)$ at focus, where wave-vectors k_x and k_y define the spatial frequencies in the x and y coordinates respectively. We will restrict our analysis to a single spatial coordinate for simplicity ($E_{IR}(x) \rightarrow E_{IR}(k_x)$). Under small angle approximation, $k_x = k \cdot sin(\theta) \approx k \cdot \theta$, and thus, $E_{IR}(k_x) \approx E_{IR}(\theta)$, where θ is the angle between the wave-vector k and the propagation direction. In case of multiple-wavelength illumination the incoming IR beam at focus is $E_{IR}(\theta, \lambda_{IR})$. The IR beam intensity is thus $I_{IR}(\theta, \lambda_{IR}) = \left|E_{IR}(\theta, \lambda_{IR})\right|^2$ and can be separated in two separate functions $I_{IR}(\theta, \lambda_{IR}) = F_{IR}(\theta) \cdot G_{IR}(\lambda_{IR})$ where $F_{IR}(\theta)$ is the angular spectrum, which is supposed to remain equal for all IR wavelengths, and $G_{IR}(\lambda_{IR})$ is the wavelength spectrum of the IR source. Both the IR beam and the pump beam will be convolved in the spatial and time frequency domain within the NL crystal. In addition and because of NCQPM, the NL crystal will show a different upconversion angular efficiency for different incoming IR wavelengths, thus making a distinct angular filtering for every illuminating wavelength. This is assessed in function $\eta(\theta, \lambda_{IR})$. The pump beam angular spectrum will be regarded as a delta function centered at 0 deg. and comprised of only one wavelength (which stems for a nearly collimated and single-frequency laser). Therefore, the accepted angular spectrum is directly the product of $I_{IR}(\theta, \lambda_{IR})$ and $\eta(\theta, \lambda_{IR})$ and it will be wavelength shifted to $\lambda_{\text{up}}^{-1} = \lambda_{IR}^{-1} + \lambda_{\text{pump}}^{-1}$. In consequence, the image at the imaging sensor is comprised of the different (but closely spaced) upconverted wavelengths and the overlap of different angular contribution at different upconverted wavelengths will compose the detected image $I_{\text{up}}(\theta)$. In a dual-wavelength laser $G_{IR}(\lambda_{IR})$ is comprised of only two wavelengths λ_1 and λ_2 of intensities a_1 and a_2 respectively. The upconverted area can be increased and its angular intensity equalized by adequately choosing the wavelength spacing $\Delta\lambda = \lambda_2 - \lambda_1$ and the intensity ratio $\alpha_I = a_2/a_1$ between the oscillating wavelengths, where a_2 and a_1 are the peak intensities at λ_2 and λ_1, respectively. From this perspective and considering NCQPM [15], the normalized upconverted

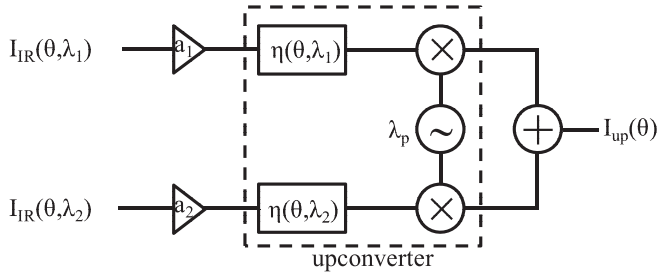

Fig. 3. Block diagram of the dual-wavelength illumination upconversion system.

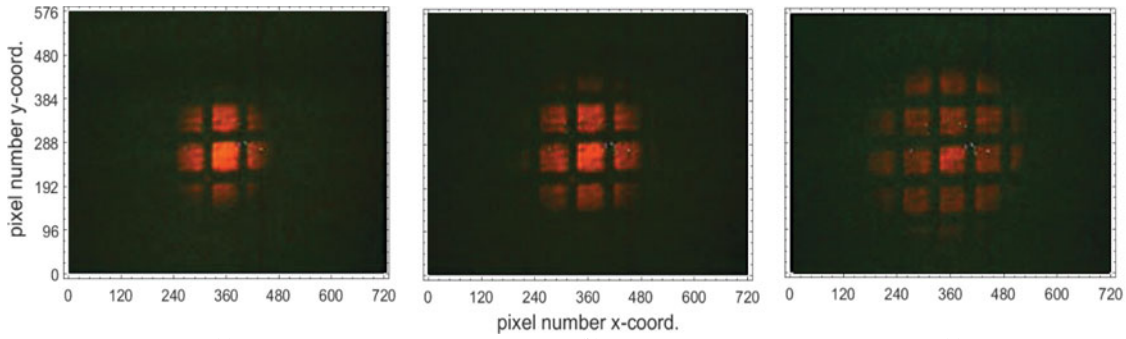

Fig. 4. Increased FOV for different wavelength spacing of the dual-wavelength laser after optimization of relative amplitudes. (a) Upconverted image for single-wavelength illumination at λ_{QPM}. (b) and (c) Upconverted images for $\Delta\lambda = 1.5$ nm and $\Delta\lambda = 2.5$ nm, respectively.

angular intensity, $I_{up}(\theta)$, may be written as

$$I_{up}(\theta) \propto F_{IR}(\theta) \int_{\lambda_1}^{\lambda_2} d\lambda_{IR} \cdot \eta(\theta, \lambda_{IR}) \cdot G_{IR}(\lambda_{IR}) = F_{IR}(\theta)[a_1 \cdot \eta(\theta, \lambda_1) + a_2 \cdot \eta(\theta, \lambda_2)]. \quad (1)$$

This equation will be employed in the following section for comparison of the measured and calculated angular response of the upconverter.

Equation (1), for the upconverter under dual-wavelength illumination, can be modeled as a system block diagram (see Fig. 3). The whole system can be regarded as a FOV equalizer, in which an enhanced FOV, in comparison with single-wavelength illumination, can be obtained real-time by weighting the dual-wavelength intensities. For outdoor applications, where the incoming light to the upconverter is expected to be reflected from surfaces, the combination of reflection and outdoor propagation may impose a certain wavelength selectivity, changing the amplitude distribution of the IR illumination spectrum and thus the angular response of the upconverter. Then, illumination comprising a broad spectrum may be difficult to equalize in real-time. As a result and in contrast to broadband illuminated upconverters, our system shows advantageous not only for brighter illumination (laser compared to broadband light), but also allows an easier mitigation of outdoor effects since only two wavelengths need to be equalized. In addition, as will be shown later in the text, using a dual-wavelength illumination source we achieved similar FOV enhancement than using broadband ASE illumination.

4. Results

In this section we will show the enhancement of the upconverter FOV under dual-wavelength laser illumination. Fig. 4 displays the increased upconverted area (FOV) for different wavelength spacing of the laser.

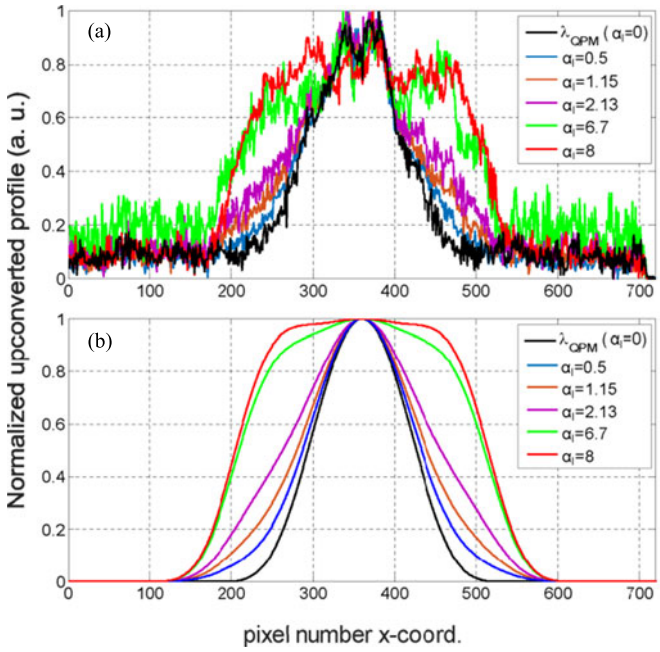

Fig. 5. (a) Experimental and (b) theoretical calculation upconverted angular response as a function of the CCD camera pixel number for $\Delta\lambda = 2.5$ nm and different intensity ratios α_I.

For these measurements, one wavelength was placed to satisfy perfect QPM ($\lambda_1 \sim \lambda_{QPM} =$ 1544.5 nm) and the other wavelength was shifted to $\lambda_2 \sim 1546$ nm [see Fig. 4(b)] and $\lambda_2 \sim$1547 nm [Fig. 4(c)] respectively. Fig. 4(a) shows the IR upconverted image for a single wavelength placed at perfect QPM and was included for comparison. The increase of FOV is clear in both Fig. 4(b) and 4(c). These figures were recorded at different (increasing) α_I for every wavelength spacing while keeping a similar upconverted power at the center of the images.

In order to evaluate the FOV enhancement we recorded in the CCD camera different pictures of the upconverted profile for a fixed $\Delta\lambda = 2.5$ nm (with $\lambda_1 \sim \lambda_{QPM} = 1544.5$ nm) and for different α_I when no target was inserted in the illumination path. In Fig. 5(a), we plot a horizontal trace at the center of the recorded upconverted profiles. The recorded images were taken for a focusing lens L1 with f1 $=$ 40 mm, a 5 mm long NL crystal, and a collecting lens L2 with f2 $=$ 75 mm at room temperature. All images were normalized to its peak value for a better visualization of the FOV enhancement. As it can be seen, for an appropriate wavelength spacing, the FOV can be enhanced by increasing the intensity of the longer wavelength, λ_2, relative to that at λ_{QPM}. In Fig. 5(b), we calculated the upconverted profiles using the experimental values of the optical components as simulation parameters in (1). A very similar behavior for the computed profiles is obtained using the model for dual-wavelength illumination in comparison to the experimentally recorded profiles. In comparison with previously obtained results [15], when employing a dual-wavelength laser as the illumination source, the measured FOV enhancement can compare to that obtained using broadband ASE illumination. For wider wavelength spacing ($\Delta\lambda$), we were unable to obtain a broad and equalized angular response. This was because the relative intensity between IR wavelengths needed to equate the angular response was high (>factor of 10) and due to gain competition in the Er-doped fiber of our laser the oscillation of λ_1 was suppressed. In addition, and regardless of the relative intensities, if the wavelength spacing is too long, a good overlap between the upconverted profiles at λ_1 and λ_2 cannot be achieved (see Fig. 6) since angular response at λ_2 shows multiple peaks (both at the center and shifted from the center).

We also evaluated the IR illumination power cost for increasing the FOV using dual-wavelength illumination relative to single-wavelength illumination. We present this cost as a power penalty. The power penalty represents the factor by which the dual-wavelength IR illumination power has to

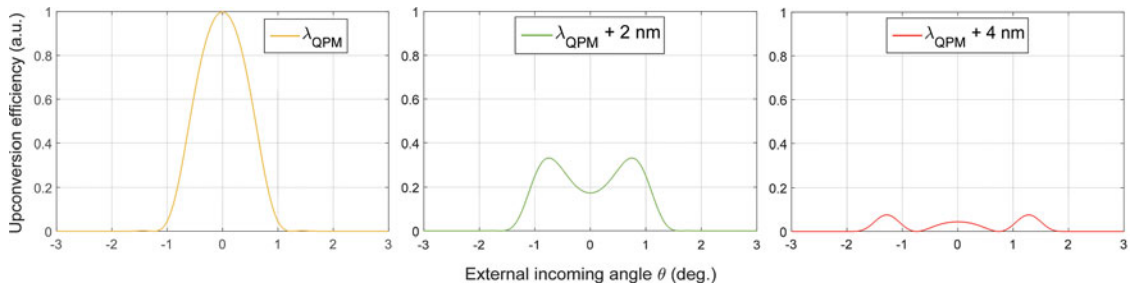

Fig. 6. Examples of calculated upconverted angular profiles at different IR illumination wavelengths. The different patterns are shown relative to λ_{QPM} which was equal to 1544.5 nm.

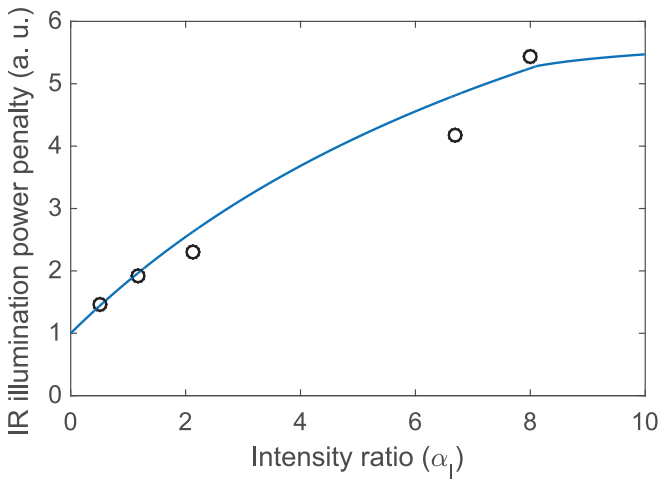

Fig. 7. Calculated and measured values of the power penalty for enhanced FOV upconversion under dual-wavelength illumination as a function of α_I for $\Delta\lambda = 2.5$ nm.

be multiplied in order to to achieve the same upconverted power at the center of the image than that available when using single-wavelength illumination at λ_{QPM} of a particular power. This power penalty will be dependent on $\Delta\lambda$ and α_I. In Fig. 7, we represent the calculated (solid line) power penalty and the measured values of the power penalty for the intensity ratios shown in Fig. 5, which was retrieved from the curves in Fig. 5(a) before normalization and at constant incoming IR power. For a $\Delta\lambda = 2.5$ nm, the widest achieved FOV required an increase of 5 in the IR illumination power.

The achieved widening of the FOV of laser radiation is of interest for outdoor application but the presented power penalty may limit its performance. For the upconversion of eyesafe signals, the increase of the illumination power could not be a restriction because of the available high-power lasers in this spectral band. Additionally, both in the eyesafe and other spectral bands, the power penalty could be overcome by means of an increase of the upconverter efficiency. This increase can be achieved by either longer NL crystal or higher intracavity SFM pump power. A longer NL crystal could be detrimental because of the inverse relation between NL crystal length and FOV, thus it would be preferable an enhancement of the intracavity SFM power.

5. Conclusions

In summary, we show that using illumination with only two laser wavelengths it is possible to produce a similar FOV enhancement as it would result in an IR image upconverter illuminated by a broadband thermal or ASE source, provided that both wavelengths and their relative power are strategically chosen, which may be regarded as a novel application of dual-wavelength lasers.

The presented model provides a good prediction of the attainable FOV for a given upconverter configuration. The power cost of enlarging the FOV has been also calculated and measured. The obtained penalty factor (~5) can be compensated either in the laser source or in the upconverter if needed. Both the possibility of FOV enhancement and the higher brightness make upconversion using dual-wavelength laser radiation an alternative compared to upconversion using broadband light sources. A step is taken towards practical infrared upconversion in outdoor applications, in particular, if IR illumination is made with pulsed Q-switched lasers thus offering longer ranges than broadband (spectrally incoherent) sources. In outdoor environments, light is expected to be reflected or scattered from object surfaces giving rise to light travelling in multiple angles, therefore widening the FOV is desirable. Furthermore, any wavelength dependence of the outdoor propagation channel, which would distort the upconverter FOV, could be easily mitigated since only two wavelengths need to be equalized.

References

[1] J. E. Midwinter, "Parametric infrared image converters," *IEEE J. Quantum Electron.*, vol. 4, no. 11, pp. 716–720, Nov. 1968.

[2] R. G. Smith, "Theory of intracavity optical second-harmonic generation," *IEEE J. Quantum Electron.*, vol. 6, no. 4, pp. 215–223, Apr. 1970.

[3] C. Pedersen, E. Karamehmedovi, J. S. Dam, and P. Tidemand-Lichtenberg, "Enhanced 2D-image upconversion using solid-state lasers," *Opt. Exp.*, vol. 17, no. 23, pp. 20885–20890, Oct. 2009.

[4] J. S. Dam, P. Tidemand-Lichtenberg, and C. Pedersen, "Room-temperature mid-infrared single-photon spectral imaging," *Nature Photon.*, vol. 6, pp. 788–793, Sep. 2012.

[5] S. Fan *et al.*, "Diffraction-limited real-time terahertz imaging by optical frequency up-conversion in a DAST crystal," *Opt. Exp.*, vol. 23, no. 6, pp. 7611–7618, Mar. 2015.

[6] C. D. Brewer, P. E. Powers, S. M. Kirkpatrick, and E. A. Watson, "Enhanced signal coupling into periodically poled lithium niobate with microlens arrays," *Appl. Opt.*, vol. 41, no. 21, pp. 4411–4415, Jul. 2002.

[7] C. Pedersen, Q. Hu, L. Hgstedt, P. Tidemand-Lichtenberg, and J. Seidelin Dam, "Non-collinear upconversion of infrared light," *Opt. Exp.*, vol. 22, no. 23, pp. 28027–28036, Nov. 2014.

[8] A. J. Torregrosa, H. Maestre, and J. Capmany, "Intra-cavity upconversion to 631 nm of images illuminated by an eye-safe ASE source at 1550 nm," *Opt. Lett.*, vol. 40, no. 22, pp. 5315–5318, Nov. 2015.

[9] J. S. Dam, C. Pedersen, and P. Tidemand-Lichtenberg, "High-resolution two-dimensional image upconversion of incoherent light," *Opt. Lett.*, vol. 35, no. 22, pp. 3796–3798, 2010.

[10] J. S. Dam, C. Pedersen, and P. Tidemand-Lichtenberg, "Theory for upconversion of incoherent images," *Opt. Exp.*, vol. 20, no. 2, pp. 1475–1482, Jan. 2012

[11] C. D. Brewer, B. D. Duncan, P. S. Maciejewski, S. M. Kirkpatrick, and E. A. Watson, "Space-bandwidth product enhancement of a monostatic, multiaperture infrared image upconversion ladar receiver incorporating periodically poled $LiNbO_3$," *Appl. Opt.*, vol. 41, pp. 2251–2262, 2002.

[12] M. I. Md Ali *et al.*, "Tapered-EDF-based Mach Zehnder interferometer for dual-wavelength fiber laser," *IEEE Photon. J.*, vol. 6, no. 5, pp. 1–9, Oct. 2014.

[13] D. Liu, N. Q. Ngo, S. C. Tjin, and X. Dong, "A dual-wavelength fiber laser sensor system for measurement of temperature and strain," *IEEE Photon. Technol. Lett.*, vol. 19, no. 15, pp. 1148–1150, Aug. 2007.

[14] H. Ahmad, F. D. Muhammad, C. H. Pua, and K. Thambiratnam, "Dual-wavelength fiber lasers for the optical generation of microwave and terahertz radiation," *IEEE J. Sel. Topics Quantum Electron.*, vol. 20, no. 5, pp. 166–173, Sep.-Oct. 2014.

[15] H. Maestre, A. J. Torregrosa, and J. Capmany, "IR Image upconversion using band-limited ASE illumination fiber sources," *Opt. Exp.*, vol. 24, no. 8, pp. 8581–8593, Apr. 2016.